Retinoic Acid Sensitivity of Triple-Negative Breast-Cancer Cells Characterized by Constitutive Activation of the NOTCH1 Pathway: The Role of RARβ

Gabriela Paroni
Istituto di Ricerche Farmacologiche Mario Negri Sede di Milano
Adriana Zanetti
Istituto di Ricerche Farmacologiche Mario Negri
Maria Monica Barzago
Istituto di Ricerche Farmacologiche Mario Negri
Mami Kurosaki
Istituto di Ricerche Farmacologiche Mario Negri Sede di Milano
Luca Guarrera
Istituto di Ricerche Farmacologiche Mario Negri Sede di Milano
Maddalena Fratelli
Istituto di Ricerche Farmacologiche Mario Negri Sede di Milano
Martina Troiani
Istituto di Ricerche Farmacologiche Mario Negri Sede di Milano
Paolo Ubezio
Istituto di Ricerche Farmacologiche Mario Negri Sede di Milano
Marco Bolis
Istituto Di Ricerche Farmacologiche Mario Negri
Arianna Vallerga
Istituto di Ricerche Farmacologiche Mario Negri Sede di Milano
Federica Biancardi
Istituto di Ricerche Farmacologiche Mario Negri Sede di Milano
Mineko Terao
Istituto di Ricerche Farmacologiche Mario Negri Sede di Milano
Enrico Garattini (enrico.garattini@marionegri.it)
Istituto Di Ricerche Farmacologiche Mario Negri

Research

Keywords: NOTCH1, retinoic acid, breast cancer, triple-negative, RARbeta

Posted Date: August 7th, 2020

DOI: https://doi.org/10.21203/rs.3.rs-53959/v1

Abstract

Background: All-trans retinoic-acid (ATRA) is a promising agent in the personalized treatment/chemo-prevention of breast-cancer. Triple-negative breast-cancer (*TNBC*) accounts for 15-20% of all mammary tumours and share common features such as a high proliferation index and a basal-like gene expression signature. In spite of this, *TNBC* is very heterogeneous and lacks effective therapeutic strategies.

Methods: We profile eighteen *TNBC* breast-cancer cell-lines for their sensitivity to the anti-proliferative action of ATRA. In addition, we perform RNA-sequencing studies in two of the most sensitive cell-lines exposed to ATRA, a γ-secretase inhibitor and combinations thereof.

Results: The only three *TNBC* cell-lines (*HCC-1599*, *MB-157* and *MDA-MB-157*) endowed with ATRA-sensitivity are characterized by constitutive activation of the NOTCH1 γ-secretase product, N1ICD and we identify the associated genetic aberrations of the NOTCH1-gene. N1ICD expression renders *HCC-1599*, *MB-157* and *MDA-MB-157* cells sensitive not only to ATRA, but also to γ-secretase inhibitors, like DAPT [N-(N-(3,5-difluorophenacetyl)-L-alanyl)-S-phenylglycine-t-butyl-ester] and PF-03084014. The anti-proliferative action of ATRA and γ-secretase inhibitors is complementary, as combinations of ATRA and DAPT or PF-03084014 cause synergistic effects. This synergism is confirmed in mouse xenografts of *HCC-1599* cells. RNA-sequencing studies performed in *HCC-1599* and *MB-157* cells exposed to ATRA and DAPT demonstrate that the two compounds act on common gene-sets, some of which belong to the NOTCH1 pathway. ATRA inhibits the growth of *HCC-1599*, *MB-157* and *MDA-MB-157* cells *via* RARα, which up-regulates several retinoid target-genes, including RARβ. RARβ induction is observed only in *HCC-1599*, *MB-157* and *MDA-MB-157* cells, as the other *TNBC* cell-lines lack ATRA-dependent stimulation of the retinoid-receptor. RARβ is a key determinant of ATRA anti-proliferative activity, as its silencing suppresses the effects exerted by the retinoid.

Conclusions: We demonstrate that ATRA exerts a significant anti-tumor action in *TNBC* cells characterized by constitutive NOTCH1 activation. We show that ATRA enhances the anti-tumor activity of γ-secretase inhibitors in an additive/synergistic manner. We support the idea that ATRA anti-proliferative activity is mediated by the Retinoid-Acid-Receptor-β (RARβ). The present study represents the basis for the design of clinical trials on the efficacy of combinations between ATRA and γ-secretase inhibitors in the treatment of patients affected by a specific subtype of *TNBC*.

Background

Triple-negative breast-cancer (*TNBC*) accounts for 15–20% of all mammary tumours and it is characterized by estrogen-receptor (*ER*), progesterone-receptor (*PgR*) and HER2-receptor negativity. Even if *TNBC* cells share common features such as a high proliferation index and a basal-like gene expression signature, this tumour type is very heterogeneous and lacks effective therapeutic strategies (1),(2).

NOTCH1 is a transmembrane receptor and it accounts for the NOTCH pathway activation observed in a minor fraction of *TNBC*s (3),(4). Normally, NOTCH1 activation requires binding to a membrane tethered

ligand on neighbouring cells, which triggers a series of proteolytic events (5),(6). The final γ-secretase-dependent cleavage of NOTCH1 causes the release and nuclear translocation of the receptor intracellular domain (N1ICD), which is an active transcription factor regulating the expression of various target genes (7),(8),(9). Activating mutations of the *NOTCH1* gene have been observed in different types of malignancies and they seem to account for approximately 13% of all *TNBC* cases (10),(11). This has raised interest in the use of γ-secretase inhibitors in the personalized treatment of different types of cancer, including *TNBC* (12). However, the use of NOTCH inhibitors as single agents in the treatment of various tumours is unlikely to be sufficient, supporting the necessity of identifying pharmacological agents boosting the activity and reducing the toxicity of these compounds.

All-trans retinoic-acid (ATRA) is a promising agent in the personalized treatment/chemo-prevention of breast-cancer (13),(14) and other tumors (15), as indicated by pre-clinical *in vitro* and *in vivo* data. Recently, we demonstrated that luminal breast-cancer cells are sensitive to the anti-tumor action of ATRA, while the basal counterparts are generally resistant (16),(17),(18). Here, we demonstrate that ATRA exerts a significant anti-tumor action in *TNBC* cells characterized by constitutive NOTCH1 activation. In addition, we show that ATRA enhances the anti-tumor activity of γ-secretase inhibitors in an additive/synergistic manner using models of this *TNBC* subtype. Finally, we support the idea that ATRA anti-proliferative activity is mediated by the Retinoic-Acid-Receptor-β (RARβ).

Methods

Cell lines and chemicals

A list of the characteristics, origin and growth conditions of the cell lines used in the study is available in Supplementary Methods. To obtain DAPT-resistant cell-lines, *MB-157* cells were cultured in the presence of the γ-secretase inhibitor (1 μM) for 40 days. Surviving cells were diluted in medium and replated at low density to isolate single-cell derived colonies. These cell cultures were grown in medium containing DAPT (1 μM) for 83 days. Two growing clones were isolated to obtain an equivalent number of DAPT-resistant cell-lines (*MB-157RCL7A* and *MB-157RCL15A*). *HCC-1599* and *MB-157* cells stably over-expressing RARβ-targeting shRNAs were obtained by lentiviral infection of constructs based on the pGreenPuro-shRNA system (SBI, System Bioscences). The sequence of the RARβ-targeting shRNAs is available in Supplementary Methods. Lentiviral infected cells were subjected to puromycin (0.5 μg/ml) selection for the isolation of the shRARβ expressing cells. The sensitivity of cell-lines to the anti-proliferative action of ATRA was evaluated with the *ATRA-score* index (see Supplementary Methods) (17).

The following chemicals were used: ATRA (Sigma-Aldrich), AM580 (Tocris), BMS961 (Tocris), UVI2003 (a kind gift of Dr. Angel De Lera, Universidade de Vigo, Spain), LE135 (Tocris), DAPT (Sigma), PF-03084014 (Pfeizer) and VP16 (SIGMA).

Cell proliferation assays and Western blot analyses

In adherent cultures, cell-growth was determined with the sulforhodamine assay (55). In suspension cultures, cell growth was evaluated with the CellTiter-Glo Luminescent Cell Viability Assay (Promega). Western blot analyses were performed as detailed in Supplementary Methods.

RNA-sequencing studies

RNA sequencing was performed as described (18), using the Illumina NextSeq500 apparatus. Alignment of high-throughput, stranded, paired-end reads (151 + 151 bp) to the reference genome (hg38), was performed using STAR-aligner, adopting the v27 release of Gencode annotations (56). Downstream analyses were carried out in the R-statistical-environment (see Supplementary Methods). The RNA-seq data are deposited in the EMBL-EBI Arrayexpress database (Accession No: E-MTAB-9203).

Determination of the NOTCH1 gene internal deletions

Exponentially growing *HCC-1599*, *MB-157* and *MDA-MB157* cells were harvested and RNA extracted using the RNeasy Mini Kit (QIAGEN). RNA was subjected to reverse transcription according to the GeneAmp® RNA PCR Core Kit (Applied Biosystems). The NOTCH1 cDNA was amplified by PCR using primers corresponding to exon 1 and exon 28 (sense: 5'-CCTGCTCTGCCTGGCGCTG-3'; antisense: 5'-CCACGAAGAACAGAAGCACA-3'). The PCR products were purified by gel electrophoresis and subjected to sequencing with the Sanger method (Eurofins Genomics srl) to identify the *NOTCH1* internal deletion breakpoint.

Luciferase and PCR assays

Cell-lines were co-transfected with the reporter plasmid pGL2HES-1/LUC (*HES1-Luc*) and the pRL-TK renilla luciferase control reporter construct. Eighteen hours after the transfection, cells were treated with DAPT (1 μM) for 24 hours. Luciferase activity was measured with the Dual-Luciferase® Reporter Assay System (Promega) on cell lysates. The expression of the NOTCH1 mRNA was evaluated with the use of a SYBR green assay (Thermo Fisher Scientific) according to the instructions of the manufacturer (Forward primer 5'CCTGCTCTGCCTGGCGCTG3', exon 1 *NOTCH1*-gene, nucleotides 283–301 of NM_017617.5; Reverse primer 5'CCACGAAGAACAGAAGCACA3', exon 28 *NOTCH1*-gene, reverse strand of nucleotides 5494–5513 of NM_017617.5).

In Vivo Studies

The experimental procedures involving animals were carried out according to the Italian legislation and the Declaration of Helsinki: The studies were approved by the internal Ethical Committee on Animal Experimentation. Treatment efficacy was evaluated from the normalized tumor-volume curves using two independent parameters: 1) tumor "growth inhibition" (GI); 2) absolute growth delay (AGD). The parameters used for the determination of the treatment efficacy are described in Supplementary Methods.

Results

ATRA sensitivity of TNBC cell-lines characterized by N1ICD expression

The *ATRA-score* is an experimental index which measures the anti-proliferative action of ATRA in cancer cells (16),(17). The low *ATRA-score* values determined in most *TNBC* cell-lines indicate that they are generally resistant to ATRA (Fig. 1A). Indeed, only three (*HCC-1599*, *MB-157* and *MDA-MB157*) of the eighteen *TNBC* cell-lines considered are endowed with high *ATRA-score* values and respond to ATRA. Two additional *TNBC* cell-lines (*HCC-1806* and *HCC-70)* present with measurable *ATRA-scores*, while all the other ones show undetectable values. Remarkably, *HCC-1599*, *MB-157* and *MDA-MB157* cell-lines are reported to be characterized by internal-deletions of the *NOTCH1*-gene (19),(20),(21),(22) which cause constitutive expression of *N1ICD*, the γ-secretase cleavage product and transcriptionally active form of NOTCH1 (23). Consistent with this, *HCC-1599*, *MB-157* and *MDA-MB157* are the only *TNBC* cell-lines expressing N1ICD (Fig. 1A).

To verify the presence of *NOTCH1*-gene alterations in *HCC-1599*, *MB-157* and *MDA-MB157* cells, we performed RNA-sequencing (*RNA-seq*) experiments. The results demonstrate an exon expression imbalance of the *NOTCH1*-gene, which indicates the presence of an internal deletion (Fig. 1B). In *HCC-1599* cells, the deletion involves exons 3–27, it eliminates the *NRR* (Negative-Regulatory-Region) from the primary *NOTCH1*-gene product (19) and it results in a gain-of-function phenotype (19),(20),(22),(24),(25). In *MB-157* and *MDA-MB157* cells, we do not detect the reported *SEC16A-NOTCH1* fusion-gene product (20), although the two cell-lines show deletion of *NOTCH1* exons 2–27. Sequencing of the PCR products (exon-1/exon-28 primers) obtained from the *HCC-1599*, *MB-157* and *MDA-MB157* RNA confirms the presence/position of the *NOTCH1*-gene internal deletions (Fig. 1C-D).

NOTCH1 role in the growth of ATRA-sensitive TNBC cell-lines

To investigate whether N1ICD activation contributes to the proliferation of *HCC-1599*, *MB-157* and *MDA-MB157* cells, we conducted studies with the γ-secretase inhibitor, *DAPT* [N-(N-(3,5-difluorophenacetyl)-L-alanyl)-S-phenylglycine-t-butyl-ester].

First, we transfected *HCC-1599*, *MB-157*, *MDA-MB157* and three *TNBC*/retinoid-insensitive (*MDA-MB231*, *HCC-38* and *MDA-MB436*) cell-lines with a reporter construct, containing a luciferase cDNA driven by the promoter of the NOTCH1 target-gene, *HES1* (26) (27). Consistent with constitutive NOTCH1 activation, *HCC-1599*, *MB-157* and *MDA-MB157* cells show high basal levels of luciferase-activity which are reduced by *DAPT* (Fig. 2A). In contrast, vehicle- and DAPT-treated *MDA-MB231*, *MDA-MB436* or *HCC-38* cells are devoid of significant luciferase-activity. In *HCC-1599*, *MB-157* and *MDA-MB157* cells, *DAPT*-dependent suppression of luciferase-activity is due to the expected inhibition of NOTCH1 cleavage into N1ICD (Fig. 2B).

Subsequently, we evaluated the anti-proliferative action of *DAPT* (1μM, 9 days). *DAPT* reduces the proliferation/survival of *HCC-1599*, *MB-157* and *MDA-MB157* cells, while it does not affect *MDA-MB231*, *MDA-MB436* and *HCC-38* cell-growth (Fig. 2C). In *HCC-1599*, *MB-157* and *MDA-MB157* cells, the action of DAPT is time- and concentration-dependent (Fig. 2D) and it is replicated with PF-03084014 (28),(29),(30), another γ-secretase inhibitor (Fig. 2E).

Cross-resistance to ATRA of DAPT-resistant cells

A comparison of the dose-response and time-dependent curves obtained in *HCC-1599*, *MB-157* and *MDA-MB157* cells with ATRA (Suppl.Fig.S1) and DAPT/PF-03084014 (Fig. 2D-E) indicates that the more a cell-line is sensitive to the retinoid, the more it responds to γ-secretase inhibitors. To support the idea, we developed *MB-157* cells with induced DAPT-resistance. Long-term culturing of *MB-157* cells in the presence of *DAPT* (1 μM) resulted in the isolation of two independent and DAPT-resistant cell-lines of clonal origin (*MB-157RCL7A* and *MB-157RCL15A*). Relative to the parental *MB-157* counterpart, *MB-157RCL7A* and *MB-157RCL15A* cells show resistance not only to DAPT, but also to ATRA (Fig. 3A). Cross-resistance is specific to ATRA, as no difference in sensitivity to other chemotherapeutics, such as VP16 (etoposide-phosphate), is observed (Fig. 3B). This cross-resistance to DAPT and ATRA supports NOTCH1 involvement in the anti-proliferative responses to the retinoid.

Synergistic anti-tumour effects of ATRA and γ-secretase inhibitors

We studied the growth-inhibitory effects of ATRA, DAPT and ATRA + DAPT combinations in retinoid-sensitive *HCC-1599/MB-157/MDA-MB157* cells and retinoid-resistant *MDA-MB231/MDA-MB436/HCC-38* cells (Fig. 3C). ATRA causes a time-dependent reduction in the growth of *HCC-1599*, *MB-157* and *MDA-MB157* cells. The anti-proliferative effect of DAPT is obvious in *HCC-1599* and *MB-157*, while it is less evident in *MDA-MB157* cells. In *MB-157* cells, ATRA + DAPT is significantly more active than ATRA or DAPT alone. A similar effect is likely to occur in *HCC-1599* cells too (Fig. 3C), although the strong anti-proliferative action of ATRA and DAPT alone masks the interaction. As for *MDA-MB157* cells, they are only mildly sensitive to DAPT (see also Fig. 2C) and the combination of ATRA + DAPT is no more effective than ATRA alone. The lack of constitutive NOTCH1 activation renders *MDA-MB231*, *MDA-MB436* and *HCC-38* cells equally resistant to DAPT, ATRA and ATRA + DAPT. In *HCC-1599* and *MB-157* cells, we evaluated the additive/synergistic nature of the potentiating effects exerted by ATRA + DAPT. Isobologram analysis (31),(32) of the dose-response data shows synergistic interactions between ATRA and DAPT in both cell-lines (Fig. 3D). In *HCC-1599* cells, the synergism is confirmed with combinations of ATRA and PF-03084014 (Suppl.Fig.S2).

To establish whether the anti-tumour action of ATRA and γ-secretase inhibitors is replicated *in vivo*, we performed experiments with xenografts of *HCC-1599* cells. Tumor-bearing animals were treated with vehicle, ATRA, PF-03084014 or ATRA + PF-03084014 for 18 days. The volume of the tumors was determined up to 15 days following treatment cessation (Fig. 4A). ATRA and PF-03084014 reduce the growth of *HCC-1599* tumours (16),(33). The ATRA + PF-03084014 combination is more effective than

each compound alone. The efficacy of the various treatments was further evaluated using "*Percentage-Growth-Inhibition*" (*%GI*) and "*Absolute-Growth-Delay*" (*AGD*). The *%GI* value is indicative of short-term anti-tumor effects, while *AGD* defines long-term delay of tumor regrowth. ATRA + PF-03084014 causes a more significant reduction of the *%GI* value than ATRA or PF-03084014 alone (Fig. 4B). At the end of all treatments, tumours invariably tend to regrow. Nevertheless and consistent with an increased long-term efficacy of the combination, the *AGD* value is higher following treatment with ATRA + PF-03084014 than ATRA or PF-03084014 alone (Fig. 4C).

The *NOTCH1*-gene internal deletion observed in *HCC-1599*, *MDA-MB157* and *MB-157* cells results in the expression of an amino-terminal deleted transmembrane precursor protein (TM-N1ICD) which is constitutively cleaved into N1ICD by γ-secretase (23). Thus, we evaluated whether ATRA, DAPT and ATRA + DAPT perturb the levels of N1ICD and TM-N1ICD. In the three cell-lines, DAPT suppresses N1ICD and increases the levels of the TM-N1ICD precursor, as a consequence of γ-secretase inhibition (Fig. 5A). ATRA reduces the amounts of N1ICD in *HCC-1599* and *MDA-MB-157* cells, while no effect is observed in the *MB-157* counterpart. Consistent with this, the levels of TM-N1ICD are reduced by the combination of ATRA + DAPT only in *HCC-1599* and *MDA-MB-157* cells. Overall the data suggest that the mechanisms underlying N1ICD down-regulation by ATRA and DAPT are different. In addition, they indicate that ATRA exerts diverse effects on the NOTCH1 pathway in *MB-157* cells relative to the *HCC-1599* and *MDA-MB-157* counterparts. Consistent with the last observation, ATRA causes a significant down-regulation of the TM-N1ICD mRNA in *HCC-1599* and *MDA-MB-157*, but not in *MB-157*, cells (Fig. 5B). Exposure of *MB-157RCL7A* and *MB-157RCL15A* cells to DAPT for 24 hours does not cause the same decrease of N1ICD intracellular levels observed in parental *MB-157* cells (Fig. 5C). Noticeably, ATRA does not alter the amounts of N1ICD in either parental or *MB-157RCL7A* and *MB-157RCL15A* cells.

To evaluate the specificity of the effects exerted by ATRA and DAPT we performed similar experiments in *MDA-MB-231*, *MDA-MB-436* and *HCC-38*, three *TNBC* cell-lines of the panel which express significant amounts of the intact NOTCH1 protein (Fig. 5D) and do not respond to ATRA (Fig. 1) or DAPT (data not shown). In the three cell-lines, DAPT and ATRA alone or in combination exert no significant effects on the constitutive amounts of NOTCH1 protein and do not induce the appearance of the N1ICD cleavage product.

Transcriptomic perturbations afforded by ATRA and DAPT alone and in combination

To get insights into the early perturbations afforded by the retinoid and the γ-secretase inhibitor on the gene-transcription profiles of *HCC-1599* and *MB-157* cells, we performed comparative *RNA-seq* studies in the two cell-lines exposed to ATRA, DAPT and ATRA + DAPT for 8 hours.

In *HCC-1599* cells, ATRA and DAPT up- and down-regulate a large number of genes (FDR < 0.05) (Suppl.TableS1; Fig. 6A). GSEA (Gene-Set-Enrichment-Analysis; HALLMARK annotations) of the genes down-regulated by ATRA and DAPT indicates that both compounds modulate the MYC-dependent gene-network negatively (Suppl.TableS2; Fig. 6B). This suggests that down-regulation of the MYC-pathway

contributes to the anti-proliferative action of the two compounds. Furthermore, both ATRA and DAPT reduce oxidative-phosphorylation, consistent with a growth-inhibitory action involving a decrease in mitochondrial activity (34). As for the up-regulated pathways, ATRA causes a significant enrichment of the "*Interferon-alpha-response*" and "*Interferon-gamma-response*" gene-networks (18). Remarkably, "*Interferon-alpha-response*" is the only up-regulated gene-network equally enriched by ATRA and DAPT (Suppl.TableS2; Fig. 6B). The *RNA-seq* data obtained in *HCC-1599* cells were further analysed to identify genes commonly up- or down-regulated by ATRA and DAPT. To this purpose, we first reduced the number of potential hits, using a threshold value for the expression fold-change caused by ATRA or DAPT (> 40%) (Suppl. Table S1; Fig. 6A). ATRA up-regulates 43% and down-regulates 28% of the genes regulated by DAPT in the same direction (Fig. 6C-D). The large fraction of common genes regulated by ATRA and DAPT is consistent with an ATRA-dependent down-regulation of the N1ICD transcription factor. The ATRA + DAPT combination causes a more sustained up- and down-regulation of 49% and 77% of these common genes, respectively (Suppl.TableS1; Fig. 6A; Fig. 6C-D). This suggests that many of the common genes are regulated by ATRA and DAPT *via* different regulatory mechanisms. We used the ATRA/DAPT common genes to generate a NOTCH1-oriented protein-protein interaction network. The results indicate that ATRA and DAPT induce the expression of 23 genes and reduce the expression of 11 genes whose products interact with NOTCH1 directly or indirectly (Suppl.Fig.S3).

In *MB-157* cells, ATRA, DAPT and ATRA + DAPT modulate the expression of a smaller number of genes than in HCC-1599 cells (Suppl.TableS1; Fig. 7A). GSEA demonstrates that ATRA up-regulates three gene-networks significantly (Fig. 7B). As observed in *HCC-1599* cells, "*Interferon-alpha-response*" is one of these top-enriched gene-networks. Surprisingly, ATRA up-regulates the MYC-dependent gene-network, which is the opposite of what is occurring in ATRA- or DAPT-treated *HCC-1599* cells and DAPT-treated *MB-157* cells. The fraction of genes commonly regulated by ATRA and DAPT (Fig. 7C) is much smaller in *MB-157* than *HCC-1599* cells (up-regulated = 29% *vs* 43%; down-regulated = 3% *vs* 28%), which supports the idea that the retinoid affects the NOTCH pathway by acting downstream of NOTCH1 expression and N1ICD activation. Co-treatment of *MB-157* cells with ATRA + DAPT enhances the action of ATRA or DAPT in the majority (up-regulated = 77%; down-regulated = 64%) of these common genes (Suppl. Table S1; Fig. 7C-D). This is consistent with the hypothesis that the majority of the ATRA/DAPT common genes are modulated by the two compounds *via* different mechanisms not only in *HCC-1599*, but also, in *MB-157* cells.

We compared the global effects of ATRA, DAPT and ATRA + DAPT on the 50 HALLMARK gene-sets in *HCC-1599* and *MB-157* cells (Fig. 7E). ATRA, DAPT and/or ATRA + DAPT down-regulate the "*E2F-targets*", "*G2M-checkpoint*" and "*MYC-targets*" gene-networks in both cell-lines. "*E2F-targets*", "*G2M-checkpoint*" down-regulation may simply be the consequence of the anti-proliferative effect afforded by the two compounds alone or in combination, while the effect on "*MYC-targets*" is likely to be of mechanistic relevance. It is also noticeable that ATRA + DAPT leads to an up-regulation of the "*Interferon-alpha-response*" and "*Interferon-gamma-response*" in both *HCC-1599* and *MB-157* cells.

Role of RARα and RARβ in ATRA anti-proliferative effects

ATRA is a pan-RAR agonist, activating the RARα, RARβ and RARγ retinoid-receptors with equal efficiency (35)·(36). To identify the RAR receptor(s) mediating the activity of ATRA in *TNBC* cell-lines, we exposed *HCC-1599*, *MB-157* and *MDA-MB157* cells to AM580 (RARα agonist), UVI2003 (RARβ agonist), BMS961 (RARγ agonist) as well as ATRA for 9 days (Fig. 8A). AM580 reduces the growth of these cell-lines in a dose-dependent manner and the effects of the RARα agonist and ATRA are quantitatively similar. In contrast, UV2003 and BMS961 do not alter the growth of *HCC-1599*, *MB-157* and *MDA-MB157* cells. Thus, ligand-dependent activation of RARα seems to be the primary determinant of ATRA-dependent action in *TNBC* cell-lines, as previously observed in luminal breast-cancer cell-lines (16).

To establish whether ATRA modulates the expression of RARα, RARβ and RARγ, we exposed six *TNBC* and six retinoid-sensitive *Luminal* breast cancer cell-lines to ATRA for 24 hours (Fig. 8B). Consistent with binding, activation and proteasome-degradation of the receptor (37), ATRA reduces the levels of RARα in almost all the cell-lines. In contrast, ATRA has no effect on the basal expression levels of RARγ in any cell-line (data not shown). As for RARβ, the product of a direct retinoid target-gene (38), no cell-line expresses detectable amounts of the receptor in basal conditions and the action of ATRA depends on the cellular phenotype and retinoid-sensitivity. In the *TNBC* context, ATRA up-regulates RARβ only in *HCC-1599*, *MB-157* and *MDA-MB157* cell-lines (Fig. 8B), indicating an association between RARβ induction and ATRA-sensitivity. In the luminal context, there is no cell-line which responds to ATRA with an induction of RARβ. Thus, RARβ is likely to play a functional role in ATRA growth-inhibitory action only in the case of *TNBC* cell-lines. With respect to this, it is remarkable that ATRA does not induce RARβ in DAPT- and retinoid-resistant *MB-157RCL7A* and *MB-157RCL15A* cells (Fig. 8C).

To support the functional relevance of RARβ induction, we silenced the retinoid-receptor in *HCC-1599* and *MB-157* cells by stable infection of retroviral constructs containing two distinct shRNAs targeting RARβ (*shRARβ-a* and *shRARβ-b*) and a control shRNA (*shCTRL*). In both *HCC-1599* and *MB-157* cell-lines, *shRARβ-a* and *shRARβ-b* suppress the ATRA-dependent induction of RARβ (Fig. 8D-E,left). In contrast, *shCTRL* does not alter the up-regulation of RARβ caused by ATRA in parental *HCC-1599* and *MB-157* cells. In these experimental conditions, RARβ knock-down induces ATRA resistance. Indeed, ATRA-dependent growth-inhibition is significantly reduced in *shRARβ-a/ shRARβ-b* infected *HCC-1599* and *MB-157* cells relative to the parental or *shCTRL* infected counterparts (Fig. 8D-E,right). The functional results obtained indicate that RARβ contributes to the growth-inhibitory action of ATRA in sensitive *TNBC* cell-lines.

ATRA-dependent RARβ induction is mediated by RARα activation, as the phenomenon is replicated by AM580 (Fig. 8F), while UV2003 and BMS961 are completely inactive (data not shown). The observation is supported by the results obtained with the RARα antagonist, ER-50891, which blocks the induction of RARβ triggered by ATRA or AM580 in *HCC-1599* cells (Fig. 8F). RARβ may contribute to ATRA anti-proliferative action in a ligand-dependent or ligand-independent manner. However, the comparative growth-inhibitory studies performed in *HCC-1599* cells with the above mentioned RAR agonists support

the idea that RARβ contributes to ATRA-dependent growth-inhibition in a ligand-independent manner (Fig. 8G). In fact, the anti-proliferative effect exerted by ATRA in *HCC-1599* cells is entirely recapitulated by the RARα agonist, AM580, which is incapable of binding and activating RARβ at the concentrations used in our experimental conditions.

Discussion

In previous studies (16),(17), we provided pre-clinical evidence that ATRA is particularly effective in *Luminal* and ER^+ breast-cancer, although a small number of *TNBC* cell-lines and primary tumours is also responsive to the retinoid. Here, we profile a large panel of *TNBC* cell-lines for their sensitivity to the growth-inhibitory action of ATRA. Among the *TNBC* cell-lines considered, only *HCC-1599*, *MB-157* and *MDA-MB157* cells show sensitivity to ATRA. The three cell-lines are characterized by specific internal deletions involving the *NOTCH1*-gene, indicating that this genetic aberration is a determinant of ATRA sensitivity in *TNBC*. In these cells, *NOTCH1*-gene internal deletion causes constitutive cleavage of the corresponding protein into the transcriptionally active N1ICD product by γ-secretase (39),(40),(41),(42). As a consequence, *HCC-1599*, *MB-157* and *MDA-MB157* cells present with high basal levels of NOTCH1-dependent transcriptional activity and require NOTCH1 activation for their growth. NOTCH1 activation renders the three cell-lines not only sensitive to ATRA, but also to γ-secretase inhibitors, like DAPT or PF-03084014, as shown in this study, and MRK-003, as demonstrated by Stoeck *et al.* (20). In *HCC-1599*, *MB-157* and *MDA-MB157* cells, the sensitivity to ATRA and DAPT or PF-03084014 is quantitatively correlated, suggesting that at least part of the retinoid anti-proliferative effect is due to perturbations of the active NOTCH1 pathway. Indeed, the transcriptomic data obtained in *HCC-1599* and *MB-157* cells indicate that ATRA modulates the expression of various genes which are equally regulated by DAPT-dependent NOTCH1 inhibition.

In *HCC-1599* cells, a large number of genes is commonly regulated by ATRA and DAPT. The phenomenon is partially explained by ATRA-dependent down-regulation of the NOTCH1 mRNA, which causes a decrease in the levels of the constitutively active N1ICD transcription factor. Transcriptional down-regulation of the *NOTCH1* gene seems to be also at the basis of the anti-proliferative action exerted by ATRA in the other N1ICD over-expressing *MDA-MB157* cell-line. In *MB-157* cells, the mechanisms underlying the effects of ATRA on the NOTCH pathway are different. Consistent with the observation that ATRA does not alter the levels of NOTCH1 mRNA, the number of genes modulated by ATRA and DAPT in a common manner is much smaller in this cell-line. Thus, ATRA is likely to target as yet unrecognized elements of the pathway laying downstream of the NOTCH1 protein in *MB-157* cells. Given the role played by NOTCH proteins in the control of Epithelial-to-Mesenchymal-Transition (EMT) (43)(44) and the homeostasis of cancer stem-cells (10),(45)(46), it is likely that ATRA down-modulates both processes (47),(48),(49). This is consistent with the differentiating effect of the retinoid and it may result in a reduction of the cancer stem-cell component of mammary tumours.

The *RNA-seq* data obtained in *HCC-1599* and *MB-157* cells exposed to ATRA, DAPT and ATRA + DAPT provide clues as to the gene-networks and pathways participating in the NOTCH1-dependent anti-tumor action of the two compounds alone or in combination. In *HCC-1599* cells, both ATRA- and DAPT-dependent down-regulation of the NOTCH1 pathway causes a substantial reduction in the expression levels of MYC and the MYC-dependent network. In this cell-line, the concordant anti-MYC action of ATRA and DAPT may be one of the major mechanisms underlying the anti-tumour action of the two compounds, as MYC is a well-known regulator of cancer cell stemness (50). Interestingly down-regulation of the MYC pathway is enhanced by the combination of ATRA + DAPT, which suggests that the two compounds exert complementary anti-MYC effects. In *MB-157* cells, DAPT causes a similar down-regulation of the MYC pathway, while ATRA treatment results in a surprising stimulation of the same pathway. The last observation is consistent with a difference in the mechanisms underlying the anti-tumour action of ATRA in *MB-157* and *HCC-1599* cells, indicating that MYC-targeting is not a major determinant of the *MB-157* growth-inhibitory response to the retinoid. In addition, the *RNA-seq* analyses provide insights as to single genes that may be functionally involved in the anti-proliferative action exerted by ATRA in *HCC-1599* and *MB-157* cells. With respect to this point, the most promising genes are the few ones which are up-or down-regulated in the two cell-lines by both ATRA and DAPT. Interestingly, 8 (*ELF3*, *FBXO32*, *FUT3*, *GRIN2D*, *KRT15*, *PRSS8*, *RNASEL*, *SCD*, *SCNN1A*, *SREBF1*, *TFAP2C*, *TINAGL1*) of the 220 genes up-regulated by both ATRA and DAPT in *HCC-1599* cells are equally induced by the two compounds in *MB-157* cells. Among the 60 genes down-regulated by the two compounds in *HCC-1599*, ANKRD1 is the only one whose expression is similarly reduced by ATRA and DAPT in *MB-157* cells. These genes are likely to be functionally involved in the anti-proliferative action exerted by ATRA. Consistent with the fact that the growth-inhibitory action of ATRA and DAPT may be associated with promotion of a differentiating process, *ELF3* (ETS-Related-Transcription-Factor-Elf-3) *SREBF1* (Sterol-Regulatory-Element-Binding-Protein-1), *FUT3* (Galactoside-3(4)-L-Fucosyltransferase), *SCD* (Acyl-CoA-Desaturase), *KRT15* (Keratin-15), *PRSS8* (Prostasin), *RNASEL* (Ribonuclease-L) are involved in fat and epithelial cell-differentiation.

From a basic and mechanistic standpoint, another important result of the study regards the specific involvement of RARβ in the anti-tumour action exerted by ATRA in retinoid-sensitive *TNBC* cells. RARβ is a well-known and direct retinoid-responsive target that can be transcribed from a promoter containing a RAR-binding sequence (51),(52),(53). In standard growth conditions, no breast-cancer cell-line shows detectable levels of the RARβ transcript or protein regardless of the basal or luminal phenotype. Here, we demonstrate that RARβ induction by ATRA is a peculiarity of the retinoid-sensitive *TNBC* cell-lines, as indicated by the results obtained in *HCC-1599*, *MDA-MB157* and *MB-157* cells. In fact, a similar induction is not observed in retinoid-resistant *TNBC* cells and any of the luminal cell-lines considered, independently of ATRA sensitivity. The reason as to why ATRA up-regulates RARβ only in the *TNBC* cellular context is unknown. However, the phenomenon may be due to regulatory mechanisms involving methylation of the promoter controlling transcription of the RARβ coding gene (54). Nevertheless, *TNBC*-specific RARβ induction is the consequence of a retinoid-dependent activation of RARα, which is constitutively expressed in all types of breast-cancer cells and it is the primary mediator of ATRA activity in mammary

tumours (16). RARβ expression contributes to the anti-proliferative action of ATRA in sensitive *TNBC* cells, as knock-down of the receptor in the *HCC-1599* and *MB-157* cell-lines induces partial resistance to the retinoid. It remains to be investigated whether RARβ action is ligand-dependent or -independent, although the data obtained with the specific RARα agonist, AM580, favour the latter hypothesis.

Conclusions

The present study has significant ramifications from both a translation and therapeutic standpoint. In fact, we identify a subset of *TNBC*s characterized by specific genetic aberrations of the *NOTCH1* gene which render the tumours markedly sensitive to the anti-proliferative action of ATRA and γ-secretase inhibitors. In addition, we demonstrate a significant cross-talk between the NOTCH and the retinoid signalling pathways which is at the basis of the synergistic growth-inhibitory effects observed with combinations of ATRA and the above mentioned γ-secretase inhibitors. The demonstrated synergistic interactions between ATRA and DAPT or PF-03084014 are of interest for the personalized treatment of this type of mammary tumour, which seems to account for approximately 3% of all *TNBC* cases [21]. Indeed, combinations of ATRA and γ-secretase inhibitors may represent rational strategies for the personalized treatment of this subset of *TNBC* patients. These combinations are likely to decrease the systemic toxicity of γ-secretase inhibitors, which is major clinical problem. In conclusion, the present study represents the basis for the design and conduction of clinical trials aimed at evaluating the efficacy of combinations between ATRA and γ-secretase inhibitors in the treatment of patients affected by TNBCs characterized by constitutive activation of the NOTCH1 pathway.

Abbreviations

ATRA = All-trans retinoic-acid; *TNBC* = Triple-negative breast-cancer; DAPT = [N-(N-(3,5-difluorophenacetyl)-L-alanyl)-S-phenylglycine-t-butyl-ester]; *ER* = Estrogen-receptor; PgR = Progesterone-receptor; N1ICD = NOTCH1 rceptor intracellular domain; RARβ = Retinoic-Acid-Receptor-β; GI = Tumor “growth inhibition”; AGD = Absolute growth delay; *RNA-seq* = RNA-sequencing; GSEA = Gene-Set-Enrichment-Analysis; EMT =Epithelial-to-Mesenchymal-Transition.

Declarations

Ethics approval and consent to participate

The manuscript contains results from in vivo studies performed on tumor xenograft bearing mice. The experimental procedures involving animals were carried out according to the Italian legislation and the Declaration of Helsinki. The studies were approved by the internal Ethical Committee on Animal Experimentation.

Consent for Publication

Not applicable

Availability of data and materials

All data generated or analysed during this study are included in this published article (and its supplementary information files). The RNA-seq data are deposited in the EMBL-EBI Arrayexpress database (Accession No: E-MTAB-9203).

Competing Interests

All the authors declare that they have no competing interests.

Funding

We would like to thank the Associazione Italiana per la Ricerca Contro il Cancro (AIRC), Individual Grant (IG) project No. 22963 to Enrico Garattini: We would also like to acknowledge funding to Enrico Garattini by the Fondazione “Italo Monzino”. The financial support provided was fundamental for the completion of the study.

Authors’ contributions

GP and EG conceived/designed the study and wrote the manuscript; AZ, MMB, MK, FB and MT performed most of the experimental work; LG, MB, AV, MT, PU and MF performed all the analyses requiring bio-computing approaches.

Acknowledgements

We would like to thank Dr. Roberta Frapolli (Department of Oncology, Istituto di Ricerche Farmacologiche Mario Negri) for the help with all the *in vivo* experiments.

References

1. Malhotra MK, Emens LA. The evolving management of metastatic triple negative breast cancer. Semin Oncol. maggio 2020;S0093775420300440.
2. Marra A, Viale G, Curigliano G. Recent advances in triple negative breast cancer: the immunotherapy era. BMC Med. dicembre 2019;17(1):90.
3. Giuli MV, Giuliani E, Screpanti I, Bellavia D, Checquolo S. Notch Signaling Activation as a Hallmark for Triple-Negative Breast Cancer Subtype. J Oncol. 11 luglio 2019;2019:1–15.
4. Shen Q, Cohen B, Zheng W, Rahbar R, Martin B, Murakami K, et al. Notch Shapes the Innate Immunophenotype in Breast Cancer. Cancer Discov. novembre 2017;7(11):1320–35.
5. McIntyre B, Asahara T, Alev C. Overview of Basic Mechanisms of Notch Signaling in Development and Disease. In: Reichrath J, Reichrath S, curatori. Notch Signaling in Embryology and Cancer [Internet]. Cham: Springer International Publishing; 2020 [citato 8 luglio 2020]. pag. 9–27. (Advances

in Experimental Medicine and Biology; vol. 1227). Available at: http://link.springer.com/10.1007/978-3-030-36422-9_2

6. Reichrath J, Reichrath S. A Snapshot of the Molecular Biology of Notch Signaling: Challenges and Promises. In: Reichrath J, Reichrath S, curatori. Notch Signaling in Embryology and Cancer [Internet]. Cham: Springer International Publishing; 2020 [citato 8 luglio 2020]. pag. 1–7. (Advances in Experimental Medicine and Biology; vol. 1227). Available at: http://link.springer.com/10.1007/978-3-030-36422-9_1
7. Moore G, Annett S, McClements L, Robson T. Top Notch Targeting Strategies in Cancer: A Detailed Overview of Recent Insights and Current Perspectives. Cells. 20 giugno 2020;9(6):1503.
8. Hossain F, Sorrentino C, Ucar DA, Peng Y, Matossian M, Wyczechowska D, et al. Notch Signaling Regulates Mitochondrial Metabolism and NF-κB Activity in Triple-Negative Breast Cancer Cells via IKKα-Dependent Non-canonical Pathways. Front Oncol. 4 dicembre 2018;8:575.
9. Yun J, Espinoza I, Pannuti A, Romero D, Martinez L, Caskey M, et al. p53 Modulates Notch Signaling in MCF-7 Breast Cancer Cells by Associating With the Notch Transcriptional Complex Via MAML1: p53 MODULATES NOTCH SIGNALING IN MCF-7 CELLS. J Cell Physiol. dicembre 2015;230(12):3115–27.
10. Giuli MV, Giuliani E, Screpanti I, Bellavia D, Checquolo S. Notch Signaling Activation as a Hallmark for Triple-Negative Breast Cancer Subtype. J Oncol [Internet]. 11 luglio 2019 [citato 12 maggio 2020];2019. Available at: https://www.ncbi.nlm.nih.gov/pmc/articles/PMC6657611/
11. Wang K, Zhang Q, Li D, Ching K, Zhang C, Zheng X, et al. PEST Domain Mutations in Notch Receptors Comprise an Oncogenic Driver Segment in Triple-Negative Breast Cancer Sensitive to a -Secretase Inhibitor. Clin Cancer Res. 15 marzo 2015;21(6):1487–96.
12. Ran Y, Hossain F, Pannuti A, Lessard CB, Ladd GZ, Jung JI, et al. γ-Secretase inhibitors in cancer clinical trials are pharmacologically and functionally distinct. EMBO Mol Med. luglio 2017;9(7):950–66.
13. Garattini E, Bolis M, Garattini SK, Fratelli M, Centritto F, Paroni G, et al. Retinoids and breast cancer: from basic studies to the clinic and back again. Cancer Treat Rev. luglio 2014;40(6):739–49.
14. Garattini E, Paroni G, Terao M. Retinoids and breast cancer: new clues to increase their activity and selectivity. Breast Cancer Res BCR. 4 settembre 2012;14(5):111.
15. Lokman NA, Ho R, Gunasegaran K, Bonner WM, Oehler MK, Ricciardelli C. Anti-tumour effects of all-trans retinoid acid on serous ovarian cancer. J Exp Clin Cancer Res. dicembre 2019;38(1):10.
16. Centritto F, Paroni G, Bolis M, Garattini SK, Kurosaki M, Barzago MM, et al. Cellular and molecular determinants of all-trans retinoic acid sensitivity in breast cancer: Luminal phenotype and RARα expression. EMBO Mol Med. luglio 2015;7(7):950–72.
17. Bolis M, Garattini E, Paroni G, Zanetti A, Kurosaki M, Castrignanò T, et al. Network-guided modeling allows tumor-type independent prediction of sensitivity to all-trans-retinoic acid. Ann Oncol Off J Eur Soc Med Oncol. 01 2017;28(3):611–21.

18. Bolis M, Paroni G, Fratelli M, Vallerga A, Guarrera L, Zanetti A, et al. All-Trans Retinoic Acid Stimulates Viral Mimicry, Interferon Responses and Antigen Presentation in Breast-Cancer Cells. Cancers. 6 maggio 2020;12(5):1169.
19. Robinson DR, Kalyana-Sundaram S, Wu Y-M, Shankar S, Cao X, Ateeq B, et al. Functionally recurrent rearrangements of the MAST kinase and Notch gene families in breast cancer. Nat Med. 20 novembre 2011;17(12):1646–51.
20. Stoeck A, Lejnine S, Truong A, Pan L, Wang H, Zang C, et al. Discovery of biomarkers predictive of GSI response in triple-negative breast cancer and adenoid cystic carcinoma. Cancer Discov. ottobre 2014;4(10):1154–67.
21. Wang K, Zhang Q, Li D, Ching K, Zhang C, Zheng X, et al. PEST domain mutations in Notch receptors comprise an oncogenic driver segment in triple-negative breast cancer sensitive to a γ-secretase inhibitor. Clin Cancer Res Off J Am Assoc Cancer Res. 15 marzo 2015;21(6):1487–96.
22. Kluk MJ, Ashworth T, Wang H, Knoechel B, Mason EF, Morgan EA, et al. Gauging NOTCH1 Activation in Cancer Using Immunohistochemistry. PloS One. 2013;8(6):e67306.
23. Kopan R, Ilagan MaXG. The Canonical Notch Signaling Pathway: Unfolding the Activation Mechanism. Cell. aprile 2009;137(2):216–33.
24. Ryan RJH, Petrovic J, Rausch DM, Zhou Y, Lareau CA, Kluk MJ, et al. A B Cell Regulome Links Notch to Downstream Oncogenic Pathways in Small B Cell Lymphomas. Cell Rep. 17 ottobre 2017;21(3):784–97.
25. Palomero T, Barnes KC, Real PJ, Glade Bender JL, Sulis ML, Murty VV, et al. CUTLL1, a novel human T-cell lymphoma cell line with t(7;9) rearrangement, aberrant NOTCH1 activation and high sensitivity to gamma-secretase inhibitors. Leukemia. luglio 2006;20(7):1279–87.
26. Schreck KC, Taylor P, Marchionni L, Gopalakrishnan V, Bar EE, Gaiano N, et al. The Notch target Hes1 directly modulates Gli1 expression and Hedgehog signaling: a potential mechanism of therapeutic resistance. Clin Cancer Res Off J Am Assoc Cancer Res. 15 dicembre 2010;16(24):6060–70.
27. Islam SS, Aboussekhra A. Sequential combination of cisplatin with eugenol targets ovarian cancer stem cells through the Notch-Hes1 signalling pathway. J Exp Clin Cancer Res. dicembre 2019;38(1):382.
28. Cui D, Dai J, Keller JM, Mizokami A, Xia S, Keller ET. Notch Pathway Inhibition Using PF-03084014, a -Secretase Inhibitor (GSI), Enhances the Antitumor Effect of Docetaxel in Prostate Cancer. Clin Cancer Res. 15 ottobre 2015;21(20):4619–29.
29. Zhang CC, Yan Z, Zong Q, Fang DD, Painter C, Zhang Q, et al. Synergistic Effect of the γ-Secretase Inhibitor PF-03084014 and Docetaxel in Breast Cancer Models. STEM CELLS Transl Med. marzo 2013;2(3):233–42.
30. Wu CX, Xu A, Zhang CC, Olson P, Chen L, Lee TK, et al. Notch Inhibitor PF-03084014 Inhibits Hepatocellular Carcinoma Growth and Metastasis via Suppression of Cancer Stemness due to Reduced Activation of Notch1–Stat3. Mol Cancer Ther. agosto 2017;16(8):1531–43.

31. Paroni G, Fratelli M, Gardini G, Bassano C, Flora M, Zanetti A, et al. Synergistic antitumor activity of lapatinib and retinoids on a novel subtype of breast cancer with coamplification of ERBB2 and RARA. Oncogene. 19 luglio 2012;31(29):3431–43.
32. Paroni G, Bolis M, Zanetti A, Ubezio P, Helin K, Staller P, et al. HER2-positive breast-cancer cell lines are sensitive to KDM5 inhibition: definition of a gene-expression model for the selection of sensitive cases. Oncogene. 11 dicembre 2018;
33. Zhang CC, Yan Z, Zong Q, Fang DD, Painter C, Zhang Q, et al. Synergistic effect of the γ-secretase inhibitor PF-03084014 and docetaxel in breast cancer models. Stem Cells Transl Med. marzo 2013;2(3):233–42.
34. Terao M, Goracci L, Celestini V, Kurosaki M, Bolis M, Di Veroli A, et al. Role of mitochondria and cardiolipins in growth inhibition of breast cancer cells by retinoic acid. J Exp Clin Cancer Res. dicembre 2019;38(1):436.
35. Garattini E, Bolis M, Garattini SK, Fratelli M, Centritto F, Paroni G, et al. Retinoids and breast cancer: from basic studies to the clinic and back again. Cancer Treat Rev. luglio 2014;40(6):739–49.
36. Chambon P. A decade of molecular biology of retinoic acid receptors. FASEB J Off Publ Fed Am Soc Exp Biol. luglio 1996;10(9):940–54.
37. Gianni M, Terao M, Kurosaki M, Paroni G, Brunelli L, Pastorelli R, et al. S100A3 a partner protein regulating the stability/activity of RARα and PML-RARα in cellular models of breast/lung cancer and acute myeloid leukemia. Oncogene. 7 dicembre 2018;
38. Balmer JE, Blomhoff R. Gene expression regulation by retinoic acid. J Lipid Res. novembre 2002;43(11):1773–808.
39. Li L, Guturi KKN, Gautreau B, Patel PS, Saad A, Morii M, et al. Ubiquitin ligase RNF8 suppresses Notch signaling to regulate mammary development and tumorigenesis. J Clin Invest. 17 settembre 2018;128(10):4525–42.
40. Shao S, Zhao X, Zhang X, Luo M, Zuo X, Huang S, et al. Notch1 signaling regulates the epithelial–mesenchymal transition and invasion of breast cancer in a Slug-dependent manner. Mol Cancer. 2015;14(1):28.
41. Azzam DJ, Zhao D, Sun J, Minn AJ, Ranganathan P, Drews-Elger K, et al. Triple negative breast cancer initiating cell subsets differ in functional and molecular characteristics and in γ-secretase inhibitor drug responses. EMBO Mol Med. ottobre 2013;5(10):1502–22.
42. Bolós V, Mira E, Martínez-Poveda B, Luxán G, Cañamero M, Martínez-A C, et al. Notch activation stimulates migration of breast cancer cells and promotes tumor growth. Breast Cancer Res. agosto 2013;15(4):R54.
43. Zhang Y, Weinberg RA. Epithelial-to-mesenchymal transition in cancer: complexity and opportunities. Front Med. agosto 2018;12(4):361–73.
44. Yi L, Zhou X, Li T, Liu P, Hai L, Tong L, et al. Notch1 signaling pathway promotes invasion, self-renewal and growth of glioma initiating cells via modulating chemokine system CXCL12/CXCR4. J Exp Clin Cancer Res. dicembre 2019;38(1):339.

45. Zhang Z, Han H, Rong Y, Zhu K, Zhu Z, Tang Z, et al. Hypoxia potentiates gemcitabine-induced stemness in pancreatic cancer cells through AKT/Notch1 signaling. J Exp Clin Cancer Res. dicembre 2018;37(1):291.
46. Xiao W, Gao Z, Duan Y, Yuan W, Ke Y. Notch signaling plays a crucial role in cancer stem-like cells maintaining stemness and mediating chemotaxis in renal cell carcinoma. J Exp Clin Cancer Res. dicembre 2017;36(1):41.
47. Shi G, Zheng X, Wu X, Wang S, Wang Y, Xing F. All- *trans* retinoic acid reverses epithelial-mesenchymal transition in paclitaxel-resistant cells by inhibiting nuclear factor kappa B and upregulating gap junctions. Cancer Sci. gennaio 2019;110(1):379–88.
48. Wu M-J, Kim MR, Chen Y-S, Yang J-Y, Chang C-J. Retinoic acid directs breast cancer cell state changes through regulation of TET2-PKCζ pathway. Oncogene. giugno 2017;36(22):3193–206.
49. Yao W, Wang L, Huang H, Li X, Wang P, Mi K, et al. All-trans retinoic acid reduces cancer stem cell-like cell-mediated resistance to gefitinib in NSCLC adenocarcinoma cells. BMC Cancer. dicembre 2020;20(1):315.
50. Litviakov N, Ibragimova M, Tsyganov M, Kazantseva P, Deryusheva I, Pevzner A, et al. Amplifications of stemness genes and the capacity of breast tumors for metastasis. Oncotarget. 26 maggio 2020;11(21):1988–2001.
51. Dollé P, Ruberte E, Leroy P, Morriss-Kay G, Chambon P. Retinoic acid receptors and cellular retinoid binding proteins. I. A systematic study of their differential pattern of transcription during mouse organogenesis. Dev Camb Engl. dicembre 1990;110(4):1133–51.
52. Zelent A, Mendelsohn C, Kastner P, Krust A, Garnier JM, Ruffenach F, et al. Differentially expressed isoforms of the mouse retinoic acid receptor beta generated by usage of two promoters and alternative splicing. EMBO J. gennaio 1991;10(1):71–81.
53. Garattini E, Bolis M, Garattini SK, Fratelli M, Centritto F, Paroni G, et al. Retinoids and breast cancer: from basic studies to the clinic and back again. Cancer Treat Rev. luglio 2014;40(6):739–49.
54. Moison C, Senamaud-Beaufort C, Fourrière L, Champion C, Ceccaldi A, Lacomme S, et al. DNA methylation associated with polycomb repression in retinoic acid receptor β silencing. FASEB J. aprile 2013;27(4):1468–78.
55. Skehan P, Storeng R, Scudiero D, Monks A, McMahon J, Vistica D, et al. New Colorimetric Cytotoxicity Assay for Anticancer-Drug Screening. JNCI J Natl Cancer Inst. 4 luglio 1990;82(13):1107–12.
56. Harrow J, Frankish A, Gonzalez JM, Tapanari E, Diekhans M, Kokocinski F, et al. GENCODE: the reference human genome annotation for The ENCODE Project. Genome Res. settembre 2012;22(9):1760–74.

Figures

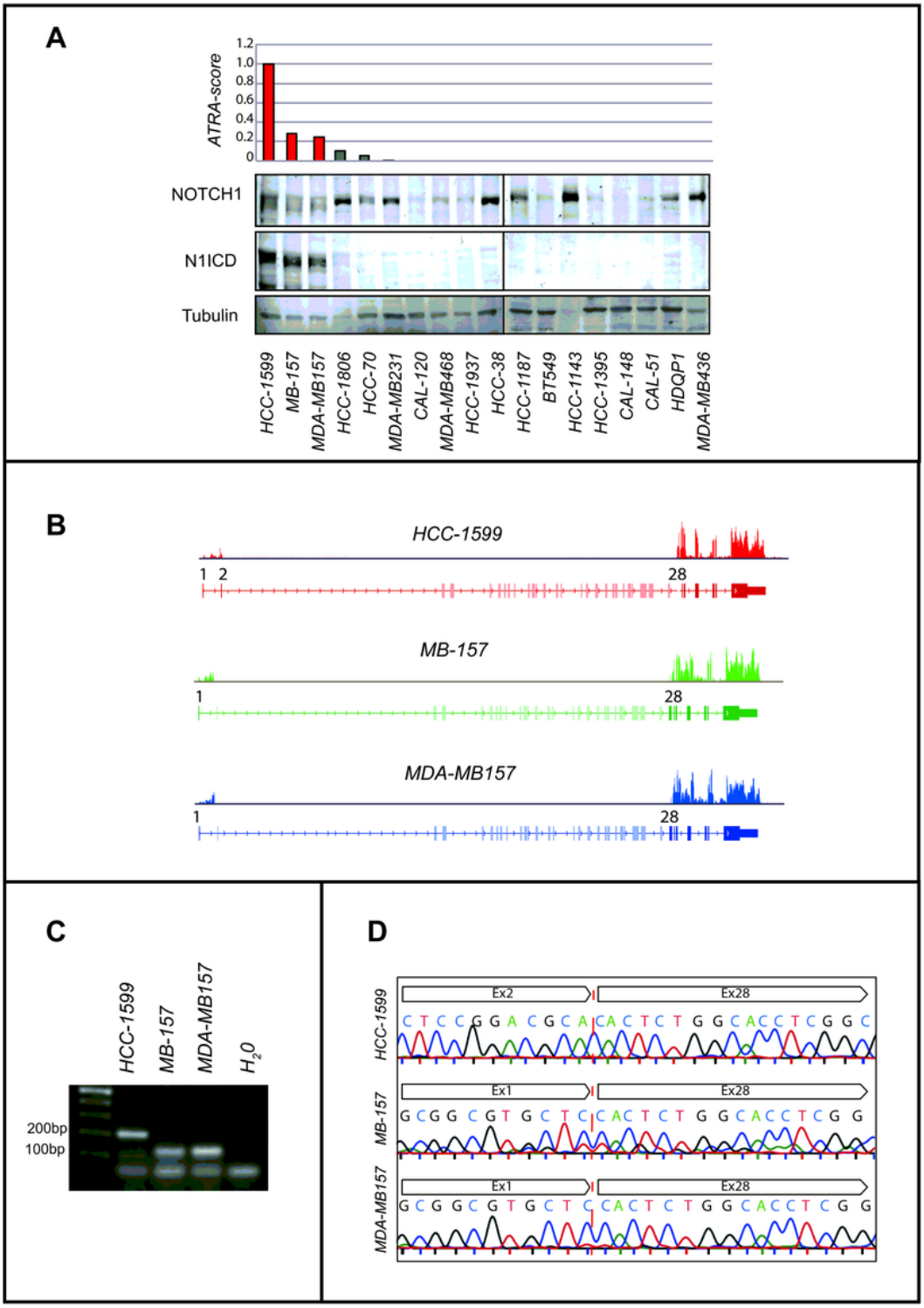

Figure 1

Association between ATRA sensitivity and N1ICD expression in TNBC cell-lines A) Upper: TNBC cell-lines are ranked in descending order according to the ATRA-score shown by the bar graph. The cell-lines characterized by internal deletions of the NOTCH1 gene are marked in red. Each ATRA-score value is representative of at least two independent experiments. Lower: The Western blots shown illustrate the levels of the NOTCH1 precursor, the N1ICD cleavage and transcriptionally active product (Val1744) of

NOTCH1 and tubulin (internal control), which were determined using specific antibodies. To perform these experiments, semi-confluent cultures of the indicated cell-lines were used. B) The panel shows density-plots illustrating the NOTCH1 gene exon expression imbalances observed in the indicated cell lines. Exons 1-34 of the NOTCH1 gene are shown. The distribution of the mapped reads aligned to the NOTCH1 gene is presented as reads per Kilobase per milion reads (RPKM). C) The indicated and exponentially growing cell-lines were harvested and subjected to RNA extraction. Following reverse-transcription, the cDNA obtained were amplified by PCR using primers corresponding to exon 1 and exon 28 of the NOTCH1 gene. Fusion amplicons of the expected size were detected. D) The panel shows the sequences of the PCR products obtained in C) and illustrates the fusion breaking points.

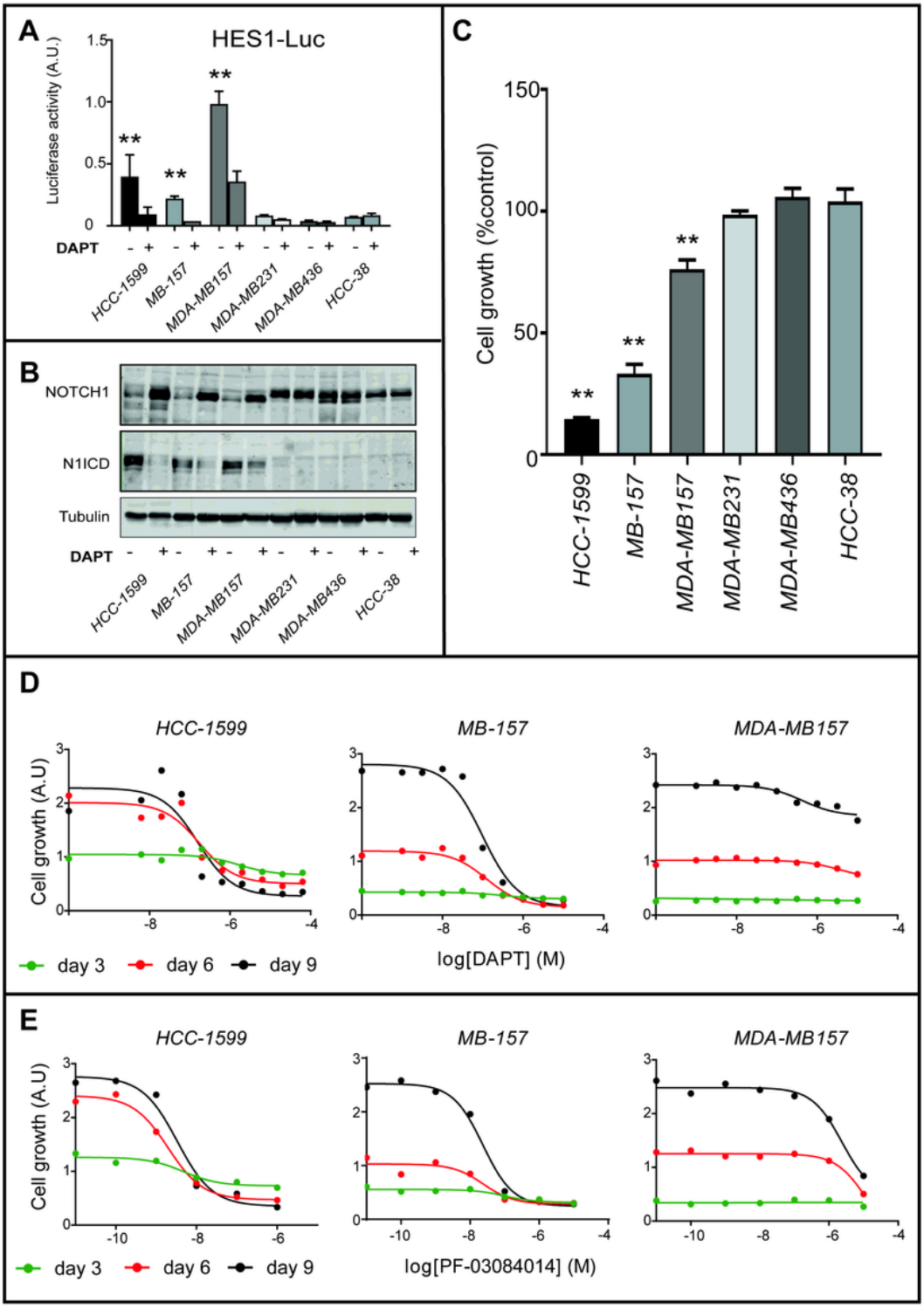

Figure 2

NOTCH1 signaling in ATRA-sensitive/ATRA-resistant TNBC cell lines and role in cellular growth (A) The indicated cell-lines were transfected with the reporter plasmid pGL2HES-1/LUC (HES1-Luc). The HES1-Luc plasmid construct contains the luciferase cDNA under the control of the promoter regulating the expression of the human NOTCH1 target-gene HES1. Eighteen hours post-transfection cells were treated with DAPT (1 μM) for 24 hours. Cell lysates were collected and analysed for luciferase activity. The pRL-

TK renilla luciferase plasmid was transfected and used as an internal control to normalise the results for the transfection efficiency. (B) The indicated cell-lines were treated with DAPT (1 μM) for 24 hours. Cell lysates were collected and analysed for NOTCH1, N1ICD or tubulin expression by Western Blot analysis using specific antibodies recognizing each protein. (C) Twenty four hours following seeding, the indicated cell lines were treated with DAPT (1 μM) for nine days. Cell-growth was determined with the use of the sulforhodamine (adherent cell-cultures, MB-157 and MDA-MB-157) assay or the CellTiter-Glo-Luminescent-Cell-Viability assay (suspension cell-cultures, HCC-1599). Cell-growth is expressed as the % of the spectrophotometric value determined in the various cell cultures exposed to vehicle (DMSO) for nine days. Each values is the mean + SD of six replicate cultures. (D) and (E) The indicated cell lines were treated with increasing concentration of the γ-secretase inhibitors, DAPT (D) or PF- 03084014 (E) for 3, 6 and 9 days. Sulforhodamine assay was performed to determine the growth of each cell-line. The panels illustrate the dose-response curves obtained with the PRISM software. Each value is the mean of 6 replicate cultures.

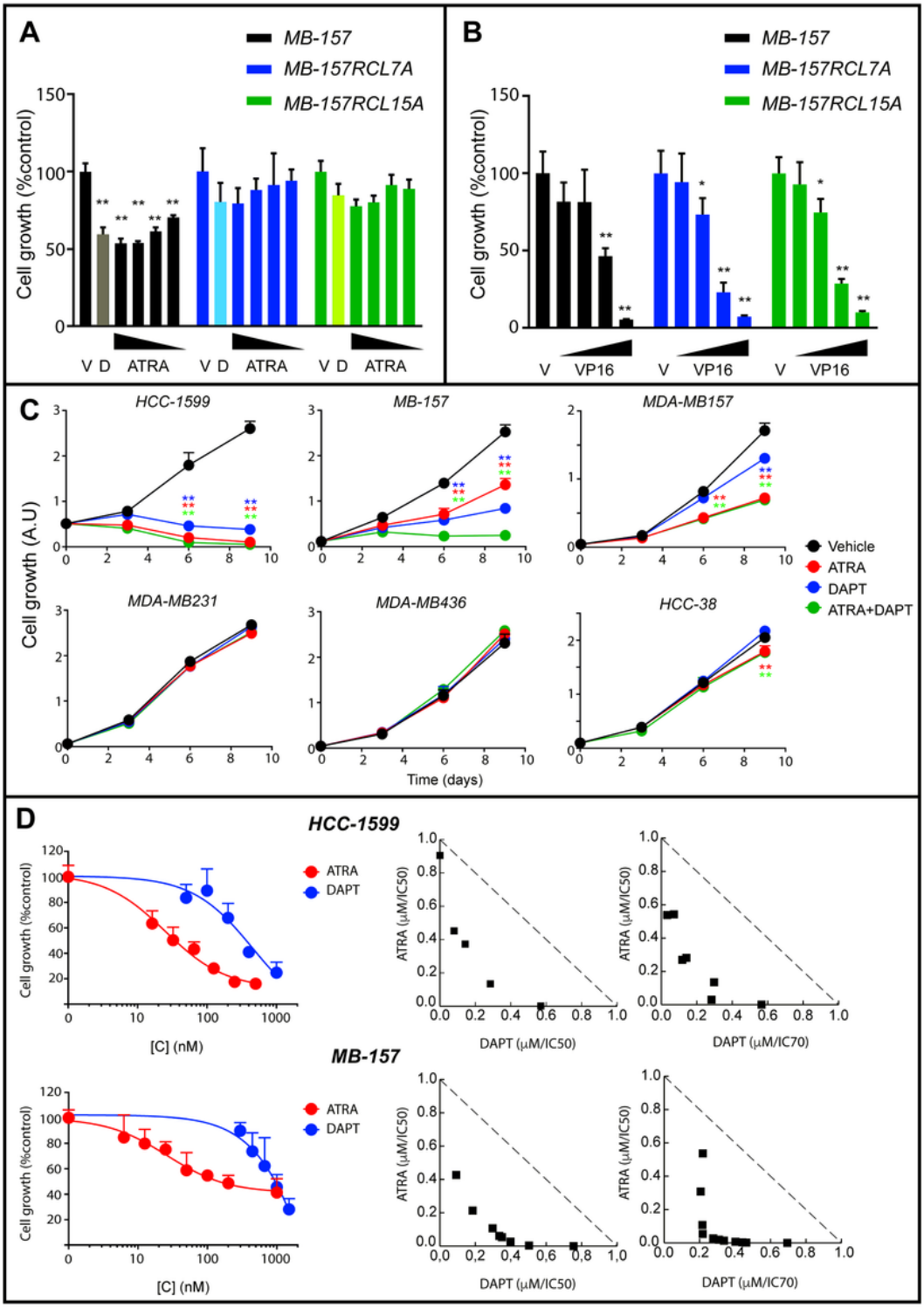

Figure 3

Effects of ATRA and DAPT alone or in combination on the growth of TNBC cell-lines characterized by constitutive N1ICD activation (A) Parental MB-157 and DAPT-resistant MB-157RCL7 and MB-157RCL15 cells were treated with vehicle (DMSO), DAPT (1µM) and decreasing concentrations of ATRA (1.0□M, 0.3□M, 0.1□M and 0.03□M) for 6 days. Cell-growth was determined with the sulforhodamine assay. Each column represents the Mean+SD of 6 replicate cultures. *Significantly lower than vehicle treated cells

(p<0.05, Student's test); *Significantly lower than vehicle treated cells (p<0.01, Student's test). (B) Parental MB-157 and DAPT-resistant MB-157RCL7 and MB-157RCL15 cells were treated with decreasing concentrations (16.0□M, 3.2□M, 0.6□M and 0.1□M) of VP16 for 3 days. Cell-growth was determined with the sulforhodamine assay. Each column represents the Mean+SD of 6 replicate cultures. *Significantly lower than vehicle treated cells (p<0.05); **Significantly lower than vehicle treated cells (p<0.01). (C) The indicated cell-lines were treated with ATRA (1μM), DAPT (1μM) or the ATRA+DAPT combination, as indicated, for 3, 6 and 9 days. Cell growth was determined with the Sulforhodamine assay (MDA-MB157 and MB-157 cells) or the CellTiter-Glo-Luminescent-Cell-Viability assay (HCC-1599 cells). Cell-growth is expressed in Arbitrary Units (A.U.) taking into account the spectrometric values determined in the various cell cultures exposed to the different stimuli for 3, 6 and 9 days. Each values is the mean + SD of six independent cultures. **Significantly lower than vehicle treated cells (p<0.01). (D) HCC-1599 and MB-157 cells were treated with vehicle (DMSO) or increasing concentrations of ATRA and DAPT alone or in combination for 9 days. Left: the panels illustrate the ATRA and DAPT dose-response curves obtained on the growth of HCC-1599 and MB157 cells. Each values is the mean + SD of six replicate cultures. Right: the panels illustrate the Isobolograms of the data obtained with combinations of ATRA and DAPT. The additivity lines separate the antagonistic (upper) from the synergistic (lower) regions.

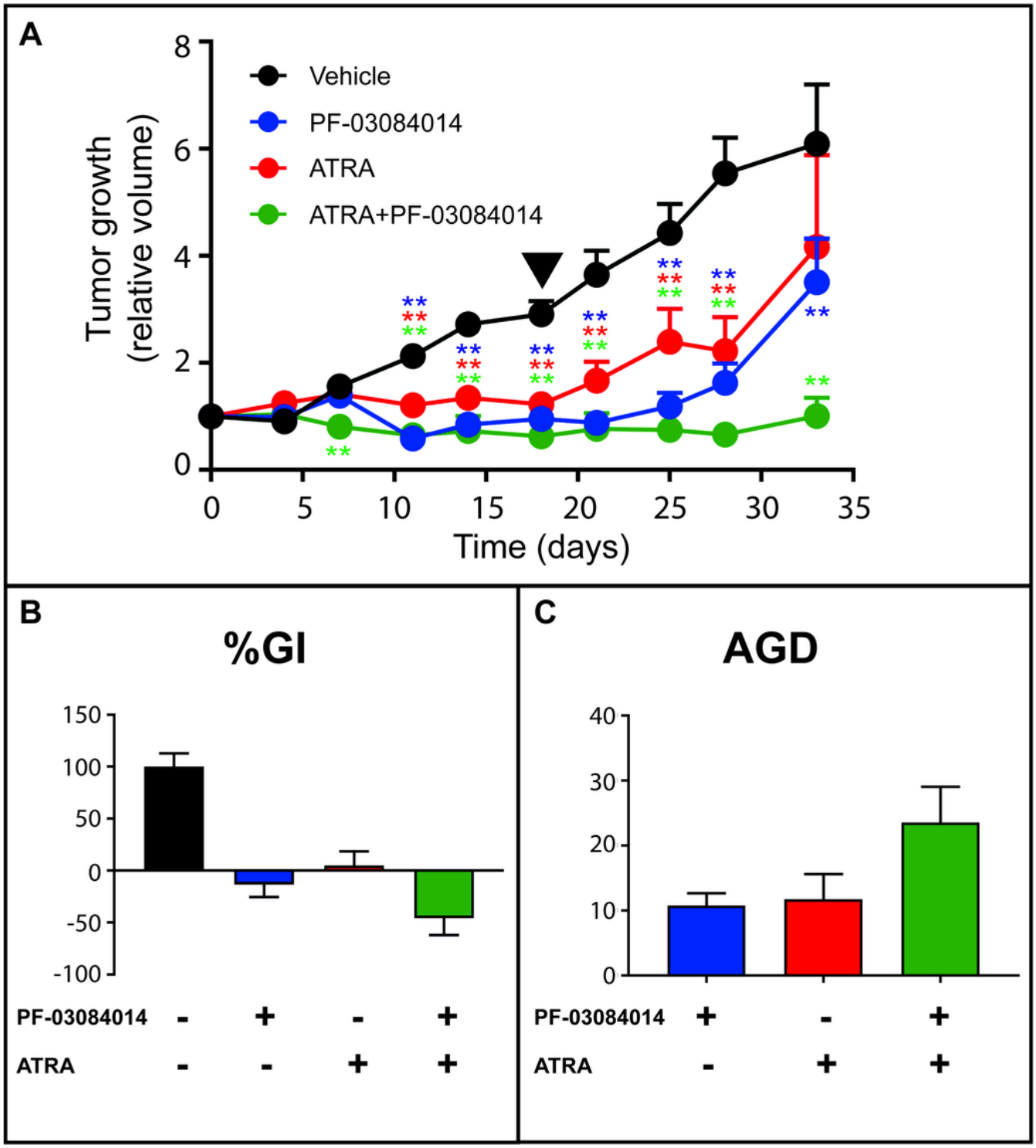

Figure 4

Anti-tumor effects of ATRA and PF-03084014 alone or in combination on the growth of HCC-1599 mouse xenograft HCC-1599 cells (1×107/animal) were injected subcutaneously on the two flanks of female SCID mice. Four days after transplantation 12 animals/experimental group were treated with: (1) vehicle; (2) PF-03084014 (90 mg/kg, twice daily per os) 5 days a week for a total of 18 days; (3) ATRA (15.0 mg/kg, once/day intraperitoneally) as in (2); (4) ATRA+PF-03084014 as in (2) and (3). The tumor volume

(TV) was determined with a caliper. (A) The panel shows the growth curve of the HCC1-599 tumor xenografts. TV values are normalized for the TV measured in the same mouse at the start of the treatment. The triangle indicates the end of the treatment. **Significantly lower relative to vehicle treated animals (p<0.01following Student's t-test). (B) and (C) Treatment efficacy is calculated from the normalized TV curves of the individual mice using two independent parameters: percentage tumor "growth inhibition" (%GI) calculated at day 18 (end of the treatment) (B) and absolute growth delay (AGD) calculated as detailed in Supplementary Methods (C). Each value is the mean+SD of 12 animals.

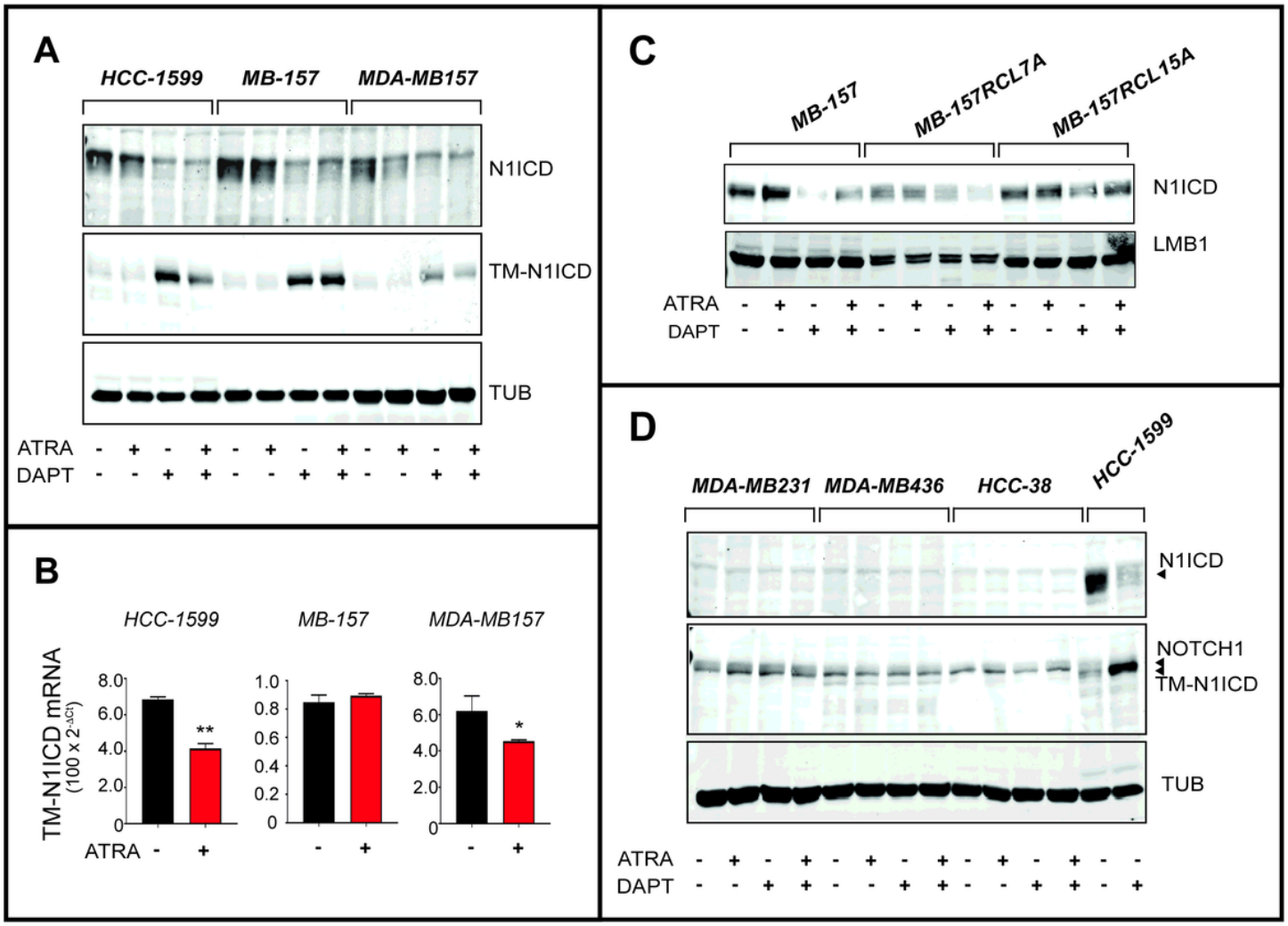

Figure 5

Effects of ATRA and DAPT on the expression of N1ICD as well as TM-N1ICD and NOTCH1 precursors in retinoid sensitive and retinoid insensitive TNBC cell-lines (A) HCC-1599, MB-157 and MDA-MB157 cells were treated with vehicle (DMSO), ATRA (1 μM), DAPT (1 μM) or the combination of the two compounds for 24 hours. Whole cell lysates were subjected to Western blot analysis for the detection of the TM-N1ICD precursor protein and the γ-secretase cleaved N1ICD product using specific antibodies. The same amount of protein was loaded in each lane and the filters were re-blotted with anti-tubulin antibodies, as indicated. (B) RNA extracted from the indicated cell-lines exposed to vehicle (DMSO) or ATRA (1 μM) for

24 hours was subjected to RT-PCR analysis using a quantitative SYBR green assay for the detection of the NOTCH1 mRNA. The results are the mean+SD of 3 replicate cell cultures. ** Significantly different ($p<0.01$, Student's t-test). * Significantly different ($p<0.05$, Student's t-test). (C) Parental MB-157 cells and DAPT-resistant MB-157RCL7A and MB-157RCL15A cells were treated with vehicle (DMSO), ATRA (1 μM), DAPT (1 μM) or the combination of the two compounds for 24 hours. Lysates were subjected to Western blot analysis for the detection of the γ-secretase cleaved N1ICD product. The same amount of protein was loaded in each lane and the filters were re-blotted with anti-laminB1(LMB1) antibodies, as indicated. (D) MDA-MB231, MDA-MB436 and HCC-38 cells were treated with vehicle (DMSO), ATRA (1 μM), DAPT (1 μM) or the combination of the two compounds for 24 hours. Lysates were subjected to Western blot analysis for the detection of the NOTCH1 precursor protein and the γ-secretase cleaved N1ICD product using specific antibodies. HCC1-599 cells were used as an internal control of the experiment.

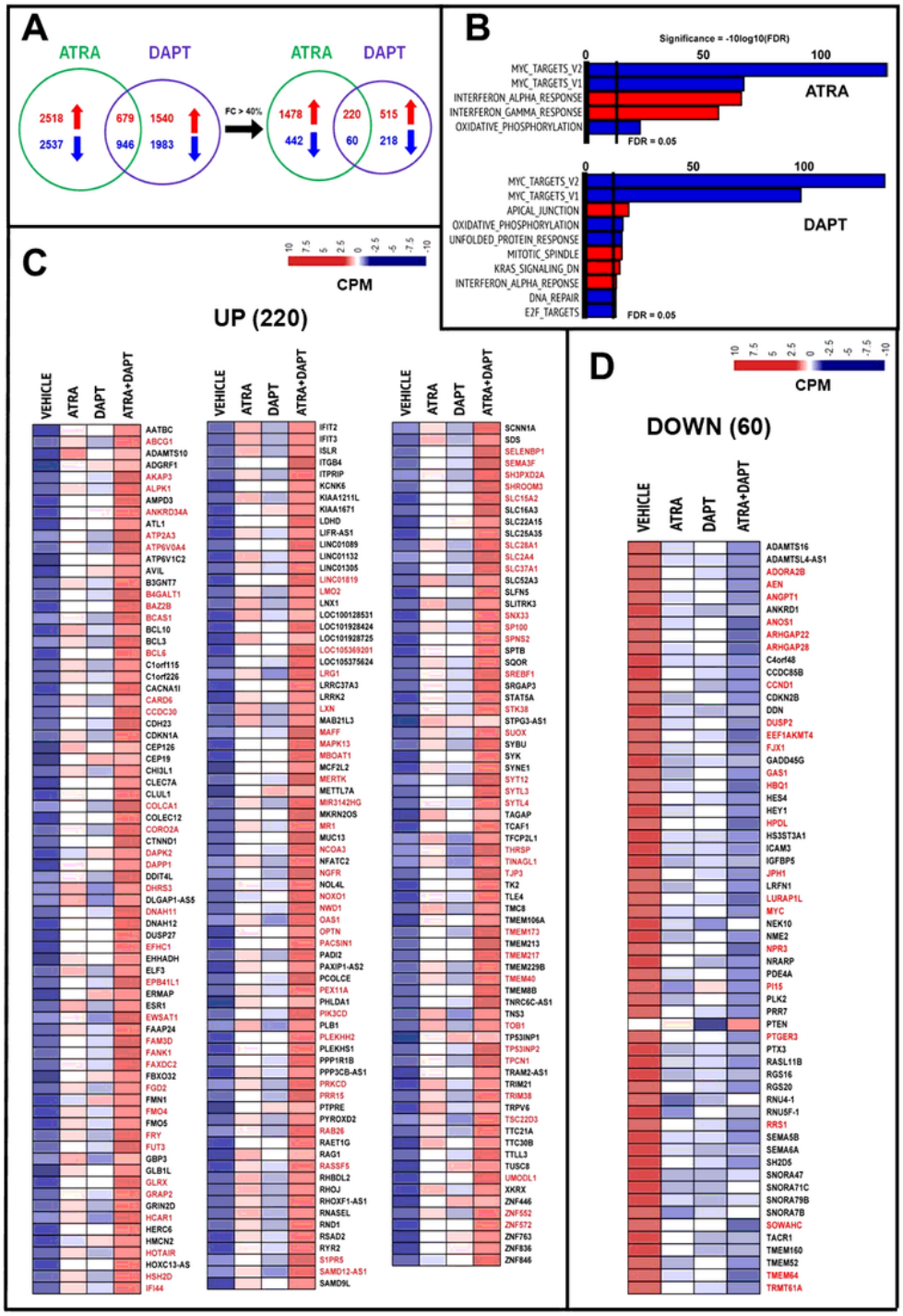

Figure 6

RNA-seq analysis of HCC-1599 cells exposed to ATRA, DAPT and ATRA+DAPT Three paired biological replicates of HCC-1599 cells were grown in DMEMF12 medium containing 5% charcolated FBS (Fetal Bovine Serum, Gibco) for 24 hours. Cells were treated with vehicle (DMSO), ATRA (1□M), DAPT (1□M) or the combination of ATRA and DAPT (ATRA+DAPT) for another 8 hours. RNA was extracted with the mRNeasy Mini Kit (QIAGEN) and subjected to RNA-seq analysis. (A) The Venn diagram on the left

illustrates the number of genes significantly up-regulated (red) and down-regulated (blue) by ATRA and DAPT. The Venn diagram on the right shows the number of genes significantly up-regulated (red) and down-regulated (blue) by ATRA and DAPT following application of the indicated threshold value (see also Suppl.TableS1). (B) The panels show the top Hallmark pathways significantly enriched for genes up-regulated (red) or down-regulated (blue) by ATRA and DAPT in HCC-1599 cells. The vertical black lines indicate the FDR (False Discovery Rate, corrected p-value<0.05) threshold values considered. (C) and (D) The heat-maps show the expression profiles of the 220 genes commonly and significantly up-regulated (C) and the 60 genes commonly and significantly down-regulated (D) by both ATRA and DAPT following application of the threshold value shown in panel (A). The effects of the ATRA+DAPT combination are also shown. The up- and down-regulation of the genes marked in red is significantly enhanced by ATRA+DAPT relative to ATRA and DAPT alone ($p<0.05$ following paired Student's t-test analysis).

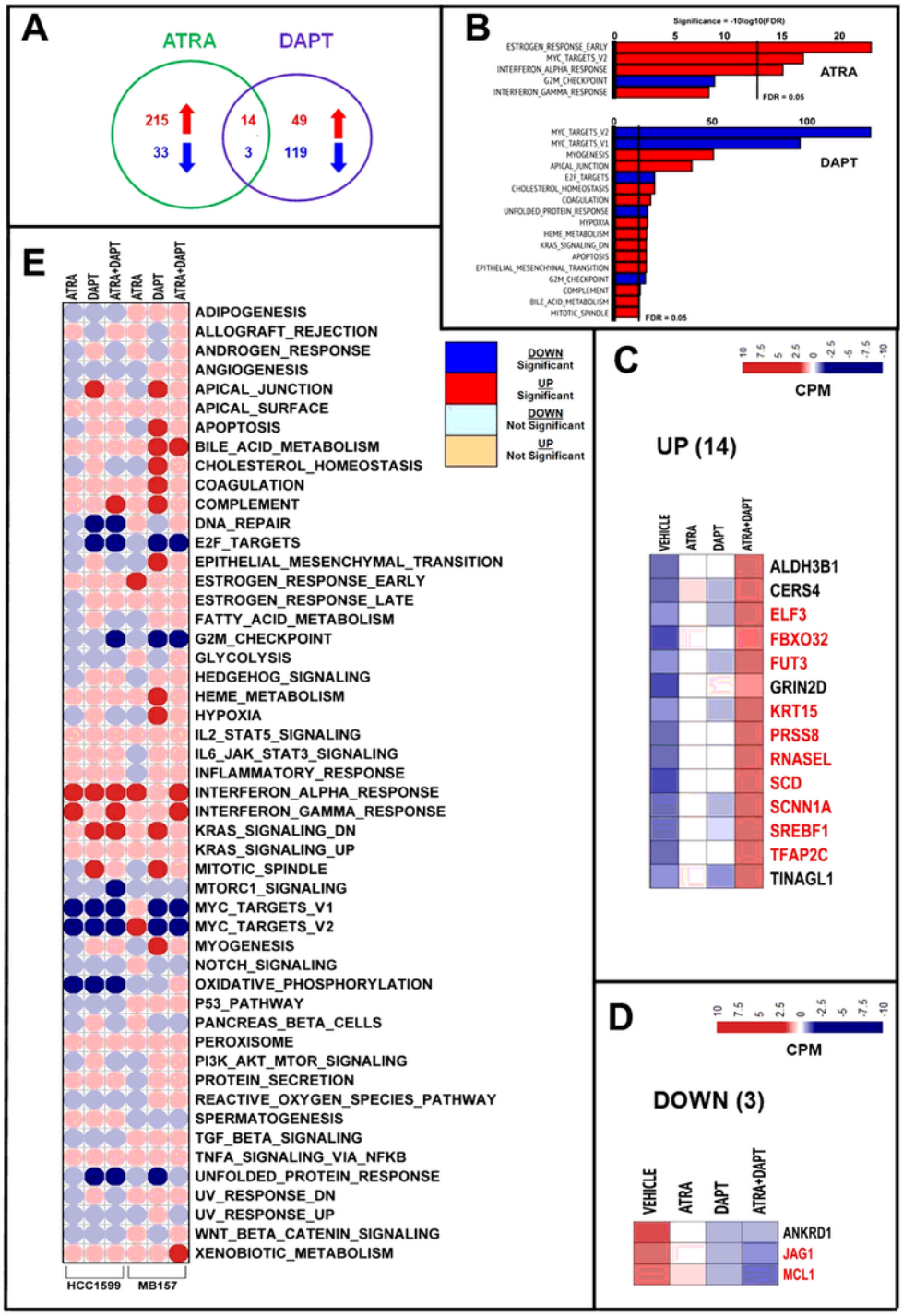

Figure 7

RNA-seq analysis of MB-157 cells exposed to ATRA, DAPT and ATRA+DAPT Three paired biological replicates of MB-157 cells were grown in DMEMF12 medium containing 5% charcolated FBS (Fetal Bovine Serum, Gibco) for 24 hours. Cells were treated with vehicle (DMSO), ATRA (1□M), DAPT (1□M) or the combination of ATRA and DAPT (ATRA+DAPT) for another 8 hours. RNA was extracted with the mRNeasy Mini Kit (QIAGEN) and subjected to RNA-seq analysis. (A) The Venn diagram illustrates the

number of genes significantly up-regulated (red) and down-regulated (blue) by ATRA and DAPT (see also Suppl.TableS1). (B) The panels show the top Hallmark pathways significantly enriched for genes up-regulated (red) or down-regulated (blue) by ATRA and DAPT in MB-157 cells, as indicated. The vertical black lines indicate the FDR (False Discovery Rate, corrected p-value<0.05) threshold values considered. (C) and (D) The heat-maps show the expression profiles of the 14 genes commonly and significantly up-regulated (C) and the 3 genes commonly and significantly down-regulated (D) by both ATRA and DAPT. The effects of the ATRA+DAPT combination are also shown. The up- and down-regulation of the genes marked in red is significantly enhanced by ATRA+DAPT relative to ATRA and DAPT alone ($p<0.05$ following paired Student's t-test analysis). (E) Corr-plot of the enrichment results obtained in HCC-1599 and MB-157 cells exposed to ATRA, DAPT and ATRA+DAPT considering the 50 Hallmark gene-sets. The analysis is based on the following comparisons: ATRA vs vehicle; DAPT vs vehicle and ATRA+DAPT vs vehicle. The red and blue circles represent the Hallmark gene-sets up- and down-regulated, respectively. The dark red and dark blue circles indicate the Hallmark gene-sets significantly up- and down-regulated with an FDR value < 0.05.

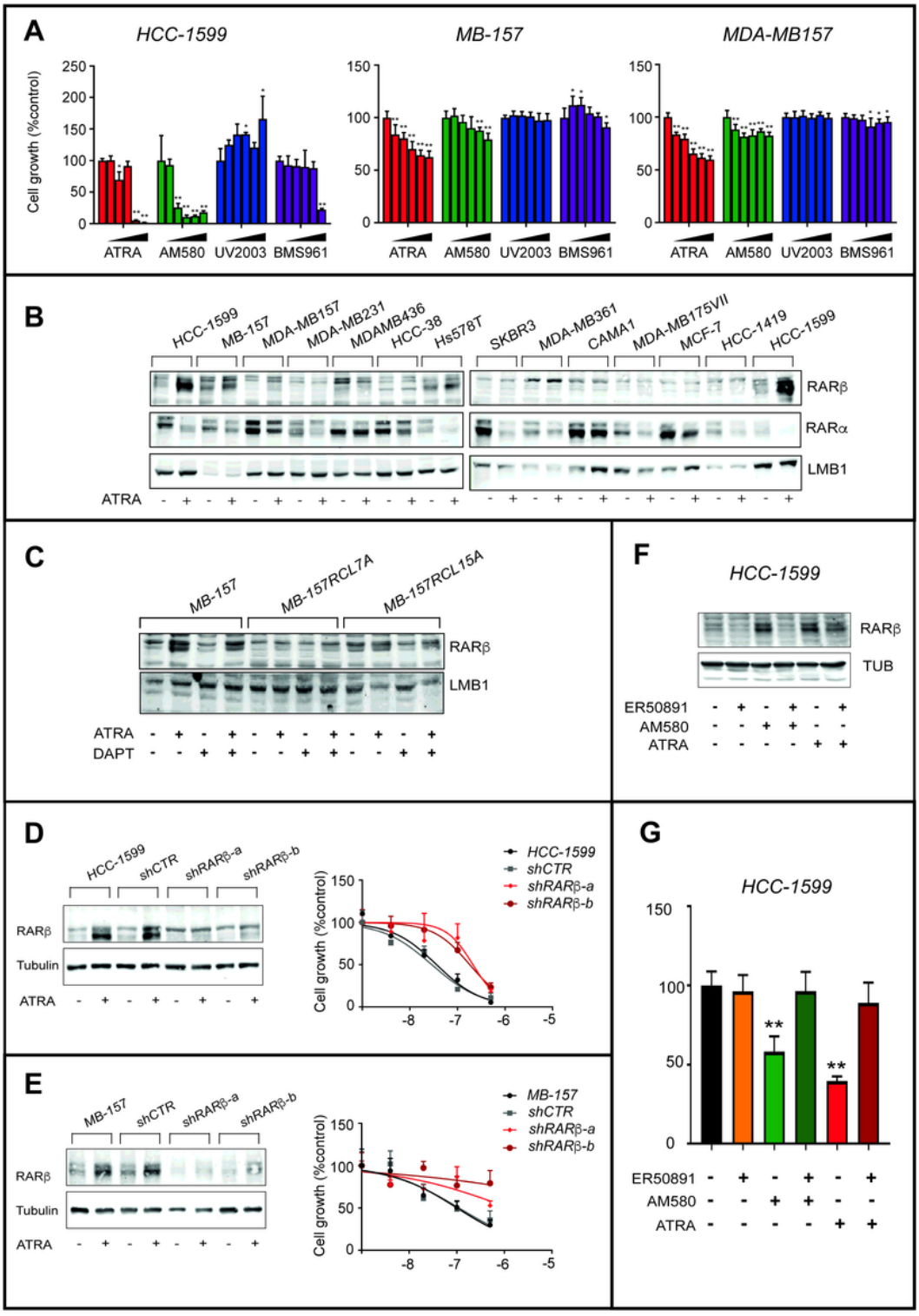

Figure 8

Involvement of RARβ in the anti-proliferative action exerted by ATRA in HCC-1599 and MB-157 cell-lines (A) At least three paired biological replicates of the indicated cell lines were challenged with vehicle (DMSO) and increasing concentrations of ATRA (1.0□M, 0.3□M, 0.1□M, 0.03□M and 0.01□M), the RARα agonist, AM580 (1.0□M, 0.3□M, 0.1□M, 0.03□M and 0.01□M), the RARβ agonist, UVI2003 (1.0□M, 0.3□M, 0.1□M, 0.03□M and 0.01□M), as well as the RARγ agonist, BMS961 (1.0□M, 0.3□M, 0.1□M, 0.03□M and

0.01□M), for 9 days. The anti-proliferative effects of each compound were determined and are illustrated by the bar-graphs. The values are expressed as the percentage of the sulforhodamine or the CellTiter-Glo-Luminescent-Cell-Viability (HCC-1599) results determined in samples treated with vehicle taken as 100. Each value is the Mean+SD of at least 3 replicates. (B) The indicated cell lines were challenged with ATRA (1μM) for 24h. Nuclear extracts were subjected to Western blot analysis for the detection of RARα and RARβ as well as LaminB1 (LMB1, loading control), using specific antibodies. (C) Parental MB-157 as well as DAPT-resistant MB-157RCL7 and MB-157RCL15 cells were treated with vehicle (DMSO), DAPT (1μM), ATRA (1□M) and the ATRA+DAPT combination for 24 hours. Nuclear extracts were subjected to Western blot analysis for the detection of RARα, RARβ and LMB1 (loading control), as in (B). (D) and (E) HCC-1599 and MB-157 cells were stably infected with lentiviral constructs expressing two distinct shRNAs against RARβ (shRARβ-a and shRARβ-b) or the empty vector (shCTR). Left panels: cell extracts were subjected to Western blot analysis for the detection of RARβ and Tubulin (loading control) using specific antibodies. Right panels: HCC-1599 and MB-157 cells were treated with increasing concentrations of ATRA (4nM, 20nM, 100nM and 500nM) for 6 days. The anti-proliferative effects of ATRA were determined with the sulforhodamine (MB-157) or CellTiter-Glo-Luminescent-Cell-Viability (HCC-1599) assays and are illustrated by the graphs. The values are expressed as the percentage of the results obtained following vehicle treatment. Each value is the Mean+SD of at least 3 replicates. (F) HCC-1599 cells were challenged with ATRA (60nM) and the RARα agonist, AM580 (60nM), in the presence or absence of the RARα antagonist ER50891(1μM) for 24 hours. Cell extracts were subjected to Western blot analysis for the detection of RARα and RARβ proteins as well as Tubulin (loading control), using specific antibodies. (G) HCC-1599 cells were treated as in (F) for 6 days. The anti-proliferative effects of each treatment were determined with the CellTiter-Glo-Luminescent-Cell-Viability assay and are illustrated by the bar-graphs. The values are expressed as the percentage of the results determined in samples treated with vehicle taken as 100. Each value is the Mean+SD of 3 replicates. ** Significantly lower relative to vehicle treated controls ($p<0.01$, Student's t-test).

Supplementary Files

This is a list of supplementary files associated with this preprint. Click to download.

- Suppl.TableS2.xlsx
- Suppl.TableS1.xlsx
- Suppl.INFOJECCR.pdf